Multi-IMU Based Alternate Navigation Frameworks: Performance & Comparison for UAS

UJJVAL N. PATEL AND **IMRAAN A. FARUQUE**

Mechanical and Aerospace Engineering Department, Oklahoma State University, Stillwater, OK 74078, USA

Corresponding author: Ujjval N. Patel (ujjval@okstate.edu)

ABSTRACT On-board state estimation is a persistent challenge to fielding unmanned aerial systems (UAS), particularly when global positioning system (GPS) measurements are not available. The dominant estimation tool remains the extended Kalman filter (EKF) applied to an inertial measurement unit (IMU). The growing availability of low-cost commercial-grade IMUs raises questions about how to best improve sensor readings into an estimate when measurements are available from multiple IMUs. This paper evaluates four different approaches to attitude estimation from multiple IMU measurements and their application in high dynamic motion. The four approaches are fusion of measurements (virtual IMU), fusion of state estimates (Federated KF), feedback fusion state estimate (Feedback Federated KF), and an EKF design incorporating the additional measurements (Augmented KF); these correspond to fusion before, within, or after state estimation. The performance of the approaches are quantified for varying IMU number theoretically and experimentally. The experiments use on-board autopilot hardware implementations of the estimators during maneuvers in a motion capture volume and flights on-board an Unmanned Aerial Systems (UAS) implementation, with the peak and root-mean-square (RMS) errors used to quantify accuracy. The RMS error results indicate that the feedback federated Kalman Filter using five IMUs returns 38% compared to general federated Kalman Filter using 37% accuracy improvement over a single IMU. This improvement compares to a 19% improvement for virtual IMU and 9% improvement for the Augmented KF respectively. These results indicate that both the Federated KF approach achieves the lowest RMS error relative to the virtual IMU and augmented KF approaches and inform the design of multi-IMU UAS pose estimators.

INDEX TERMS State estimation, Kalman filters, unmanned aerial systems, inertial navigation, quaternions, Bortz estimator, multi-IMU, inertial measurement unit, autopilot, attitude estimation.

I. INTRODUCTION

In recent years, the growth in commercial applications of Unmanned Aerial Systems (UAS) have been supported by the availability of inertial measurement units (IMUs). IMU manufacturing processing improvements have resulted in reductions of size, price and power consumption, combined with software and algorithm development including sensor calibration, measurement integration, sensor fusion. These advances have all supported the proliferation of consumer grade IMUs in low-cost UAS platforms.

The associate editor coordinating the review of this manuscript and approving it for publication was Jiankang Zhang.

As commercial UAS applications extend to becoming measurement system platforms, there is a need for improved state estimation accuracy without significant cost increase. A key use of the estimates are as a reference for atmospheric wind inference algorithms that use precise state information to estimate local wind conditions [1]. When the wind estimates are used as inputs to developing local weather forecasting algorithms that have sensitive dependence on initial conditions, the precision of state estimation must be improved beyond the tolerances acceptable for UAS navigation. Given the decreasing cost of consumer and industrial grade IMUs, multi-IMU estimators geared towards improving accuracy can yield a significant improvement in accuracy at a low cost

and serve as a foundation to long term dead reckoning, real-time accurate wind and environment parameter estimations, and potentially provide tactical grade applications using consumer grade sensors.

There are multiple options to fusing sensor information, and this paper examines the fusion problem by considering four basic approaches: fusing the measurements (i.e., before estimation), higher order estimator design (i.e., within estimation), fusing the state estimates (i.e., after estimation), and fusing the state estimates with feedback. The main objectives of this paper are to:

- Outline the four classes of multi-IMU frameworks for improving state estimation accuracy.
- Define underlying local attitude filters to be integrated with the different multi-IMU estimation approaches.
- Test the performance of the system considered in software and analyze the results as a comparison of performance improvements against a reference.

In this study, four general multi IMU state estimation frameworks are considered to fuse state estimates using two separate local Kalman filters. We then analyze and quantify the performance of the sensor fusion by implementing the multi-IMU state estimation using a hardware example with five IMUs.

The remainder of this paper is structured as follows. Section II reviews previous work done in multi-IMU based navigation and their applications to different fields not limited to aviation. Section III defines the typical non linear system to be estimated using multi-IMU formulations. In Section IV, four different fusion approaches are considered and evaluated. Section V expands on the local filter design needed to implement the multi-IMU formulation. Section VI outlines the experimental setup and implementation to evaluate and compare the performances of all the multi-IMU formulations and discusses the outcome of the paper.

II. PREVIOUS WORK

The idea of using multiple IMUs to achieve performance improvement has been used in different industries. Reference [2] used an ad-hoc Kalman filter integrating two IMUs for marine navigational purposes. Position estimation accuracy from multi-IMU approaches can significantly exceed the single IMU case, as indicated by [3], which compared satellite launcher position estimation and showed the three IMU case reduced error by 54% relative to the single IMU case. Reference [4] applied the [3] framework to an integrated navigation system that includes a traditional inertial navigation system (INS) with auxiliary IMU sensors.

Multiple researches such as the ones discussed in the papers [5]–[10] have been conducted to improve noise characteristics using multi-IMU sensor arrays rather than focusing on sensor fusion for estimation improvement. One of such method is considered in this research by fusing the measurements into a synthetic IMU output or "virtual IMU" having reduced noise statistics [11]. This method is non domain specific as categorised in [12]. This means that this methods can be used for any application regardless of system.

Previous work in the aviation industry using multiple IMUs in a navigation system has been dominated by a focus on their applications as a part of estimator health monitoring or fault detection. In these treatments, their purpose is to facilitate sensor (IMU) or estimator fault detection rather than improve estimate accuracy. Examples of this work is outlined in [13]. Marine applications have also used multi-IMU (2-IMUs) for fault detection and redundancy in case of a single IMU failure such as in [14].

Some results are available for position-only multi-IMU pedestrian navigation architectures when a global positioning system (GPS) measurement is also available. References [15], and [6] evaluated multiple and experimentally evaluated the architectures using five IMUs, which showed position estimate accuracy improvements exceed 30%.

Other studies that are more closely related to this research have focused on dynamic systems analyzed all frameworks individually rather than an extensive framework comparison [16], [17]. Where as other researches focused on the orientation of sensor placement [18]–[21]. Despite the work in this area to develop multi-IMU fusion approaches, experimental data for dynamic systems on their comparative performance remains sparse. As a result, the question of which approaches are best implement in an airborne UAS platform requiring higher accuracy is not yet answered quantitatively for high rate dynamic systems. This work begins to answer that by systematically outlining and comparing four estimation strategies based on previous literature and most commonly referenced [3], [11], [15], [22]. The results include both theoretical and experimental results of the approaches implemented in an on-board UAS autopilot and on the same measurements, allowing direct comparison.

III. PROBLEM STATEMENT

A general nonlinear system may be written in discrete dynamics form as

$$x_{k+1} = f(x_k, u_k) + w_k$$
$$y_{i,k} = h(x_k, u_k) + v_{i,k}, \quad (1)$$

where the initial state x_0 is unknown Gaussian variable; i.e., $x_0 \sim \mathcal{N}(\mu_0, P_0)$. The state vector $x_k \in \mathbb{R}^n$, and control vector $u_k \in \mathbb{R}^m$. The measurement vector $y_{i,k} \in \mathbb{R}^p$ with i being the ith sensor where $i = 1, 2, 3, \ldots, N$. The nonlinear dynamic and measurement function are represented by $f(\cdot) \in \mathbb{R}^n$ and $h(\cdot) \in \mathbb{R}^p$ respectively. The system process and measurement noise vectors $w_k \sim \mathcal{N}(0, Q)$ and $v_{i,k} \sim \mathcal{N}(0, R)$ assume zero mean Gaussian noise with covariance matrices $Q \in \mathbb{R}^{n \times n}$ and $R_i \in \mathbb{R}^{p \times p}$.

$$E \left(\begin{bmatrix} w \\ v_1 \\ v_2 \\ \vdots \\ v_N \end{bmatrix} \begin{bmatrix} w \\ v_1 \\ v_2 \\ \vdots \\ v_N \end{bmatrix}^T \right) = \begin{bmatrix} Q & 0 & 0 & 0 & 0 \\ 0 & R_1 & 0 & 0 & 0 \\ 0 & 0 & R_2 & 0 & 0 \\ 0 & 0 & 0 & \ddots & 0 \\ 0 & 0 & 0 & 0 & R_N \end{bmatrix} \quad (2)$$

For the given problem our aim is to find the optimal (in a minimum variance sense) fusion technique to obtain $\hat{x}_m(k)$ based on measurements $y_i(k)$, where $i = 1, 2, \ldots, N$ which satisfies following minimum performance requirements:

1) The fused state estimate is unbiased.
2) Optimal weights for sensor fusion minimize the trace of error covariance.

This study explores four approaches to this problem, which are referred to as the federated Kalman filter (FKF), The augmented Kalman filter (AKF), and the virtual inertial measurement unit (vIMU) approach.

IV. ESTIMATOR FUSION FORMULATION AND ERROR ANALYSIS

In this section, the four different estimation fusion formulation are evaluated for their performance in multi IMU framework as shown in Fig. (1). The virtual IMU method is most consistent with previous single-sensor estimates and this configuration used to define a theoretical "ideal" improvement benchmark which is used to evaluate the performance of actual implementation. All four frameworks described are globally optimal or sub-optimal depending on embodiment constraints [23]–[25].

A. VIRTUAL INERTIAL MEASUREMENT UNIT (vIMU)

The virtual IMU approach first unifies the n sensor measurements into a single measurement having improved noise characteristics [15], [26] by an arithmetic mean of measurements from each sensor. The approach then applies a traditional single IMU sensor estimator and uses its output as the fused state estimates, as shown in Fig. 1(a). More precisely, the estimator is constructed as

$$x_{k+1} = \Phi_k x_k + \Gamma_k w_k$$
$$y_k = \frac{1}{N} \sum_{i=1}^{N} y_{i,k} \tag{3}$$

where x_k is a n dimensional state, with Φ_k and Γ_k being discrete state and noise transition matrix respectively. $y_{i,k}$ denotes the measurements obtained from each sensor with N being total number of sensors.

An idealized estimate of the improvement in state estimation for the VIMU approach may be derived by applying Bernoulli's theorem, or the weak law of large numbers [27], which describes how a sequence of probabilities converges. Under the assumption of multiple measurements being independent variables drawn from the same distribution, the law describes the behavior of the average of the results obtained from a large number of trials. The mean result approaches the distribution's expected value and application of the Chebyshev inequality [28] shows the result will tend to become closer to the expected value as more trials are performed. Assuming the measurements $\hat{x}_1, \hat{x}_2, \ldots, \hat{x}_N$ are N independent state estimates of equal variance ($\sigma_{\hat{x}_N}^2$), the

sample mean $\hat{x}$ approaches the true state as $N \longrightarrow \infty$.

$$\text{var}(\hat{x}_m) = \text{var}\left(\frac{\hat{x}_1 + \hat{x}_2 + \cdots + \hat{x}_N}{N}\right)$$
$$= \text{var}\left(\frac{\hat{x}_1}{N}\right) + \text{var}\left(\frac{\hat{x}_2}{N}\right) + \cdots + \text{var}\left(\frac{\hat{x}_N}{N}\right)$$
$$= \frac{\sigma_{\hat{x}_1}^2}{N^2} + \frac{\sigma_{\hat{x}_2}^2}{N^2} + \cdots + \frac{\sigma_{\hat{x}_N}^2}{N^2}$$
$$= \frac{\sigma_{\hat{x}_N}^2}{N}$$

Given, for any $\epsilon > 0$

$$\lim_{N \to \infty} P\left[\left|\frac{\hat{x}_m}{N}| - \hat{x}_N\right| \geq \epsilon\right] \to 0$$

From Chebyshev's inequality,

$$P[|\hat{x}_m - \hat{x}| \geq \epsilon] \leq \frac{\text{var}(\hat{x}_m)}{\epsilon^2} = \frac{\sigma_{\hat{x}_N}^2}{N\epsilon^2}.$$

Thus,

$$\lim_{N \to \infty} P[|\hat{x}_m - \hat{x}_N| \geq \epsilon] = 0,$$

giving the ideal improvement in state estimation one can expect to be

$$\sigma_{\hat{x}_m} = \sqrt{\text{var}(\hat{x})}, \quad \text{or}$$
$$\sigma_{\hat{x}_m} = \frac{\sigma_{\hat{x}_N}}{\sqrt{N}}.$$

This idealized estimate accuracy improvement, shown in Fig. 2, serves as a theoretical contour with which to compare the measured performance improvement of the multi IMU estimators.

B. AUGMENTED KALMAN FILTER

The augmented Kalman filter approach consists of designing an extended Kalman filter for the problem using the augmented measurement vector

$$y = \begin{bmatrix} y_1 \\ y_2 \\ \vdots \\ y_N \end{bmatrix}$$

consisting of all N available measurements as shown in Fig. 1(b). The corresponding discrete measurement equation may be written as

$$y_k = H_k \hat{x}_k \tag{4}$$

where,

$$H_k = \begin{bmatrix} H_{1,k} \\ H_{2,k} \\ \vdots \\ H_{N,k} \end{bmatrix} \tag{5}$$
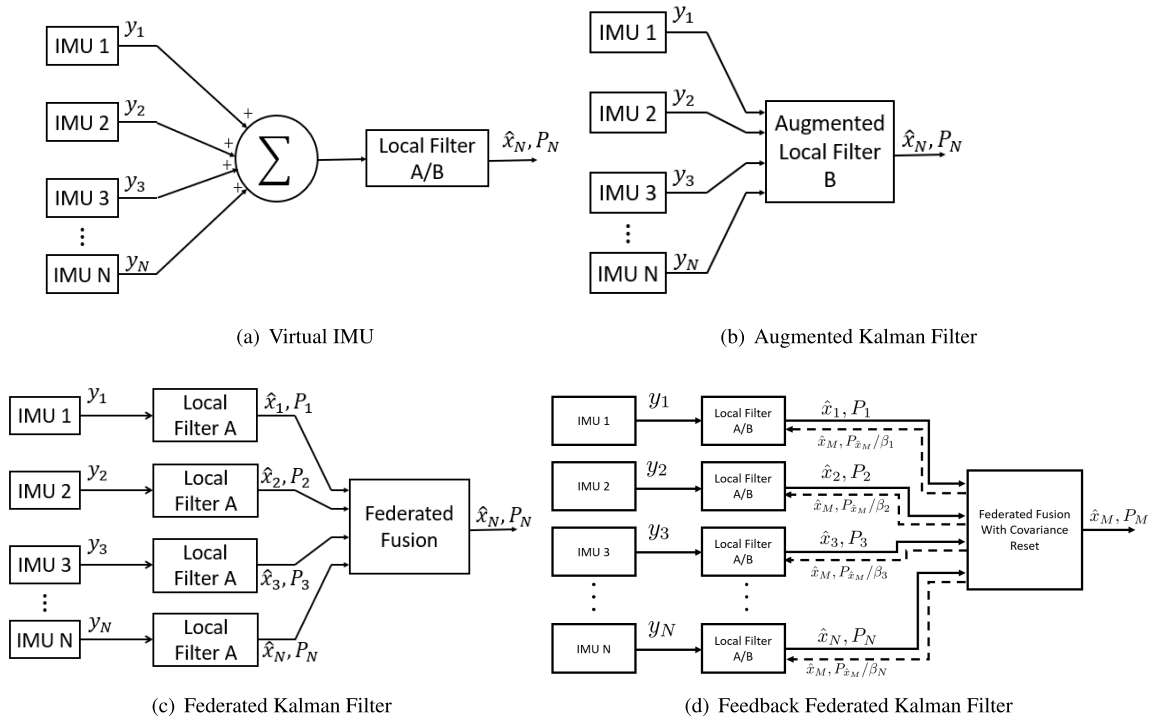
(a) Virtual IMU

(b) Augmented Kalman Filter

(c) Federated Kalman Filter

(d) Feedback Federated Kalman Filter

FIGURE 1. Estimation fusion architectures considered.

with $H_1, H_2, \ldots, H_n$ corresponds to their respective measurement matrix for each sensor (IMUs for scope of this research).

The nine parameter augmented estimation consists of a traditional propagation and measurement correction step [25]. The Augmented Kalman Filter differs from the typical single-IMU Kalman filter only in the measurement equation and measurement correction step, where it uses all gyro and accelerometer measurements. For the five IMU case tested in Section VI, the system has 30 observations and operates at the same frequency as the incoming observations. The observability matrix in equation (5) is full rank and the AKF is a semi-optimal estimator [25].

C. FEDERATED KALMAN FILTER (FKF)
In the federated Kalman Filter approach shown in Fig. 1(c), N individual local state estimators are implemented, each having a single sensor (IMU) as an input and each generating both a state estimate $\hat{x}_i$ and corresponding covariance matrix $P_i, i = 1, \ldots, N$. As defined by Carlson and Berarducci [29], the approach

1) Scales the initial values of local filter covariance and process noise matrices.
2) Performs local time propagation and measurement update process.
3) Combines the updated local information into a global information.
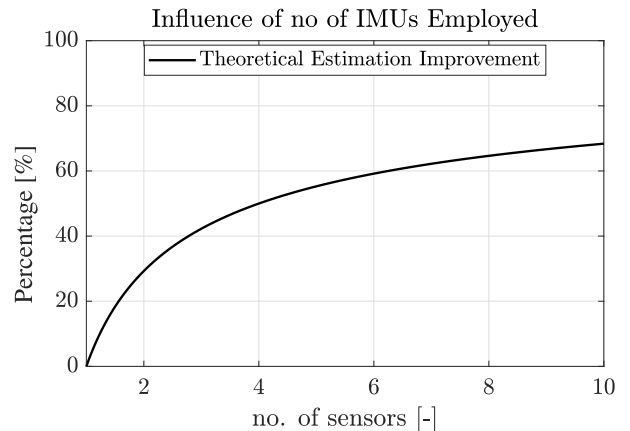4) Resets local information to the scaled global information.

FIGURE 2. Percentage improvement in estimation with numbers of IMUs employed.

The state estimates are then fused into a single state estimate $\hat{x}_m$ using a covariance-based weighting as

$$\hat{x}_m = P_m \left(\sum_{i=1}^{N} P_i^{-1} \hat{x}_i \right), \tag{6}$$

$$P_m = \left(\sum_{i=1}^{N} P_i^{-1} \right)^{-1}. \tag{7}$$

The FKF approach yields a globally optimal estimate [23] and its error covariance follows the additive equation (Eqn. (7)).

D. FEEDBACK FEDERATED KALMAN FILTER (FFKF)

This approach is an extension of the Federated Kalman Filter with an added step of resetting the state and covariance to the fused parameters for all local filters with scaled multi-IMU covariance propagation using scaling factor β. Eqn. (8)-(11) represents the estimation routine. This estimation method should perform better than general FKF as it propagates higher accuracy fused state and scaled covariance.

$$\hat{x}_m = P_m \left(\sum_{i=1}^{N} \beta_i P_i^{-1} x_i \right), \tag{8}$$

$$P_m = \left(\sum_{i=1}^{N} \beta_i P_i^{-1} \right)^{-1}, \tag{9}$$

$$\sum_{i=1}^{N} \beta_i = 1, \tag{10}$$

$$Q_m^{-1} = \sum_{i=1}^{N} \beta_i Q_i^{-1}. \tag{11}$$

The drawback of this approach is that it could diverge if not properly tuned. One of the parameter that could result in divergence is the choice of β. This method of information sharing through a scaled feedback follows all the information conservation principle outlaid by Carlson and Berarducci [29] and followed by Brown and Sturza [24] shows that this method of state estimation follows the same optimality as the general federated Kalman filter.

The choice of β depends on a lot of factors such as the quality of sensors, placement of the sensors, manufacturing methods, etc. For this study we use the variance measurement based on (Appendix B) and [30] to conclude that the sensors used in this papers are similar in performance and this approach is more direct and reduces computational complexity and hence, $\beta = 1/N$ is a reasonable assumption to make.

V. LOCAL FILTER FORMULATION

Due to difference in implementation requirements for all frameworks described in this paper (i.e. AKF formulation measurements from sensors cannot be used during priori step), we need to use two different local filter methods. We use Bortz equation (13) to obtain an Extended Kalman Filter framework for attitude estimation to implement Virtual Sensor Method and Federated Kalman Filter, and we will use six degree of freedom (6DOF) kinematic equation to obtain a Extended Kalman Filter to be use to implement Augmented Kalman Filter. Both local filter formulation are derived from base sensor dynamics so the difference in performance just due to local filter is not observed.

A. ATTITUDE ESTIMATION USING BORTZ EQUATION

The local attitude estimator algorithm used in this paper is based on the symmetry-exploiting method proposed in Bortz [31]. For any attitude described by a quaternion q, there

exists a rotation vector ϕ such that

$$q(\phi) = \begin{bmatrix} \frac{1}{2} \left(\frac{\sin(\gamma/2)}{\gamma/2} \right) \phi \\ \cos(\gamma/2) \end{bmatrix} \in \mathbb{R}^{4 \times 1}. \tag{12}$$

The Bortz equation for rotation error as a function of angular rate ω may be written as

$$\dot{\phi} = \omega + \frac{1}{2}\phi \times \omega + \frac{1}{\gamma^2} \left[1 - \frac{\gamma \sin \gamma}{2(1 - \cos \gamma)} \right] \phi \times (\phi \times \omega), \tag{13}$$

where ϕ is the rotation vector in Eqn. (12) and $\gamma = |\phi|$. Assuming small γ and neglecting higher order terms, Eqn. 13 becomes

$$\dot{\phi} = \omega + \frac{1}{2}\phi \times \omega. \tag{14}$$

Equation 14 now can be augmented with constant bias states b to form the state equation

$$\begin{bmatrix} \dot{\phi} \\ \dot{b} \end{bmatrix} = \begin{bmatrix} \omega + \frac{1}{2}\phi \times \omega \\ 0_{3 \times 1} \end{bmatrix}. \tag{15}$$

Both EKF framework were derived by Pittelkau [25] for a recursive implementation and using the same notation for multiplicative product operator ($\otimes$), where *priori* state estimate in quaternion form can be estimates as per

$$\begin{bmatrix} \delta\hat{\phi}_k \\ \delta\hat{b}_k \end{bmatrix} = \begin{bmatrix} \delta\hat{\phi}_{k-1} \\ \delta\hat{b}_{k-1} \end{bmatrix}$$

with

$$\begin{bmatrix} \delta\hat{\phi}_{k-1} \\ \delta\hat{b}_{k-1} \end{bmatrix} = \begin{bmatrix} 0 \\ 0 \end{bmatrix}$$

and the estimate quaternion $\hat{q}$ for that state is obtained as

$$\hat{q}_k^- = q(\hat{\phi}_k^-) \otimes \hat{q}_{k-1}^+.$$

Now, considering a vector $v^s = [v_x^s, v_y^s, v_z^s]^T$ in the sensor reference measurement. The measurement function for a three-axis magnetometer can be formulated as

$$y = v^s + \epsilon, \tag{16}$$

with ϵ as additive noise. The three-axis magnetometer is sufficient to generate an orientation estimate based on the magnetic field, which will be used in the correction step. All three axes are measured, thus $\partial h / \partial (v^s)^T = I$. The 3D measurement sensitivity matrix $H^{(3)} \in \mathbb{R}^{3 \times 3}$ is given by

$$H^{(3)} = \frac{\partial v^s}{\partial \phi^T} \bigg|_{\phi=0} = T_b^s v^b$$

where T_b^s is a body-to-sensor transformation matrix and v^b is measurement in body frame.

The predicted measurement is than given by equation 16

$$\hat{y}_k = \hat{v}_b^s = q(\hat{\phi}_s^b)v^s$$

where $q(\hat{\phi}_s^b)$ is the *priori* estimated attitude and the residual is simply $v_k = y_k - \hat{y}_k$. Using this information we can use

the sub-optimal Kalman Gain to obtain the *posteriori* state estimates using measurements obtained from magnetometer readings as a standalone correction to the EKF output from the IMU estimates.

$$K_k = P_{k-1}H_k^T(H_kP_{k-1}H_k^T + R_k)^{-1}$$
$$\hat{\phi}_k^+ = \hat{\phi}_k^- - K_k(y_k - \hat{y}_k),$$

where, K is the Kalman gain and P is the covariance matrix. Now, with updated state estimate in quaternion form is given by

$$\hat{q}_k^+ = q(\hat{\phi}_k^+) \otimes \hat{q}_{k-1}^-.$$

Similarly, the formulation outlined by Koshravian [32] can be used to integrate information about state estimates using heterogeneous sensors like LIDAR, optic-flow, etc.

B. ATTITUDE ESTIMATION USING KINEMATIC EQUATION

Using formulation for attitude estimation by Kane and David [33] using quaternions we can represent the non linear system observer in equation (1) using gyroscope angular measurement to describe the quaternion dynamics and bias as random walk as:

$$\begin{bmatrix} \dot{q} \\ \dot{b}^\omega \end{bmatrix} = \begin{bmatrix} \frac{1}{2}S(\omega - b^\omega)q \\ 0 + v \end{bmatrix} = \begin{bmatrix} \frac{1}{2}S(q)(\omega - b^\omega) \\ 0 + v \end{bmatrix} \quad (17)$$

and

$$S(\omega) = \begin{bmatrix} 0 & -\omega_x & -\omega_y & -\omega_z \\ \omega_x & 0 & \omega_z & -\omega_y \\ \omega_y & -\omega_z & 0 & \omega_x \\ \omega_z & \omega_y & -\omega_x & 0 \end{bmatrix}$$

$$S(q) = \begin{bmatrix} -q_1 & -q_2 & -q_3 \\ q_0 & -q_3 & q_2 \\ q_3 & q_0 & -q_1 \\ -q_2 & q_1 & q_0 \end{bmatrix},$$

where v is noise, $q = [q_0, q_1, q_2, q_3]$ are quaternion representing the orientation of the vehicle, and $\omega = [\omega_x, \omega_y, \omega_z]$ are bias corrected gyro measurements. The accelerometer and magnetometer are then used as measurement to compensate for drift from gyro bias error as:

$$\begin{bmatrix} y_h^a \\ y_h^m \end{bmatrix} = \begin{bmatrix} C_L^I(a_e - g) + e^a \\ C_L^I B^N + e^m \end{bmatrix}, \quad (18)$$

with C_L^I defines the rotation from body L to intermediate reference frame I.

Taking the nonlinear system's Jacobian to linearize and discretize with time step of $dt = t_k - t_{k-1}$ gives

$$\underbrace{\begin{bmatrix} q \\ b^\omega \end{bmatrix}_k}_{x_k} = \underbrace{\begin{bmatrix} I_{4\times4} & -\frac{dt}{2}S(q) \\ 0_{3\times4} & I_{3\times3} \end{bmatrix}_{k-1}}_{\Phi_{k-1}} \underbrace{\begin{bmatrix} q \\ b^\omega \end{bmatrix}_{k-1}}_{x_{k-1}} \quad (19)$$

and

$$\underbrace{\begin{bmatrix} y_h^a \\ y_h^m \end{bmatrix}_k}_{y_k} = \underbrace{\begin{bmatrix} C_a & 0_{3\times3} \\ C_m & 0_{3\times3} \end{bmatrix}_k}_{H_k} \underbrace{\begin{bmatrix} q \\ b^\omega \end{bmatrix}_k}_{x_k} \quad (20)$$
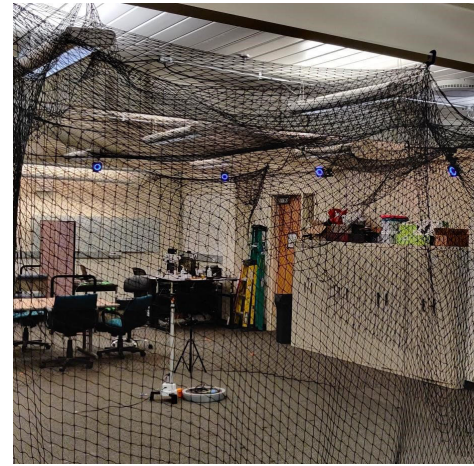

FIGURE 3. Experimental setup, including 24 camera motion capture system.

with,

$$C_a = -2 \begin{bmatrix} -q_2 & q_3 & -q_0 & q_1 \\ q_1 & q_0 & q_3 & q_2 \\ q_0 & -q_1 & -q_2 & q_3 \end{bmatrix}_k$$

$$C_m = -2 \begin{bmatrix} q_3 & q_2 & q_1 & q_0 \\ q_0 & -q_1 & q_2 & -q_3 \\ -q_1 & -q_0 & q_3 & q_2 \end{bmatrix}_k$$

Now the optimal estimate for the state vector can be obtained using Kalman filter using time update and observation update. The time update process of the Kalman filter is independent and is written as outlined by Yang and Gao [34]:

$$\hat{x}_{k|k-1} = \Phi_{k-1}\hat{x}_{k-1|k-1}$$
$$P_{k|k-1} = \Phi_{k-1}P_{k-1|k-1}\Phi_{k-1}^T + Q_k. \quad (21)$$

The observation update equation of the Kalman filter is expressed as:

$$K_{k|k} = \frac{P_{k|k-1}H_k^T}{(H_kP_{k|k-1}H_k^T + R_k)}$$
$$P_{k|k} = (I - K_{k|k}H_k)P_{k|k-1}$$
$$\hat{x}_{k|k} = \hat{x}_{k|k-1} + K_{k|k}(y_k - H_k\hat{x}_{k|k-1}) \quad (22)$$

where $\hat{x}_{k|k-1}$ is the a priori state estimation, $\hat{x}_{k|k}$ is the a posteriori state estimation, $K_{k|k}$ is the Kalman gain matrix of the Kalman filter, $P_{k|k-1}$ is the a priori covariance matrix of the state vector, $P_{k|k}$ is the a posteriori covariance matrix of the state vector, R_k is the covariance matrix of the measurement noise vector, Q_k is the covariance matrix of the process noise and Φ_k is the system transition matrix from time $k - 1$ to time k.

C. ESTIMATION RUN

To evaluate the performance of all four estimation fusion routine, estimators had to track a manual oscillatory input in range of $-90°$ to $+90°$ (which includes gimbal lock singularity) at an angular rate of about $36°/sec$ in each axis. The data
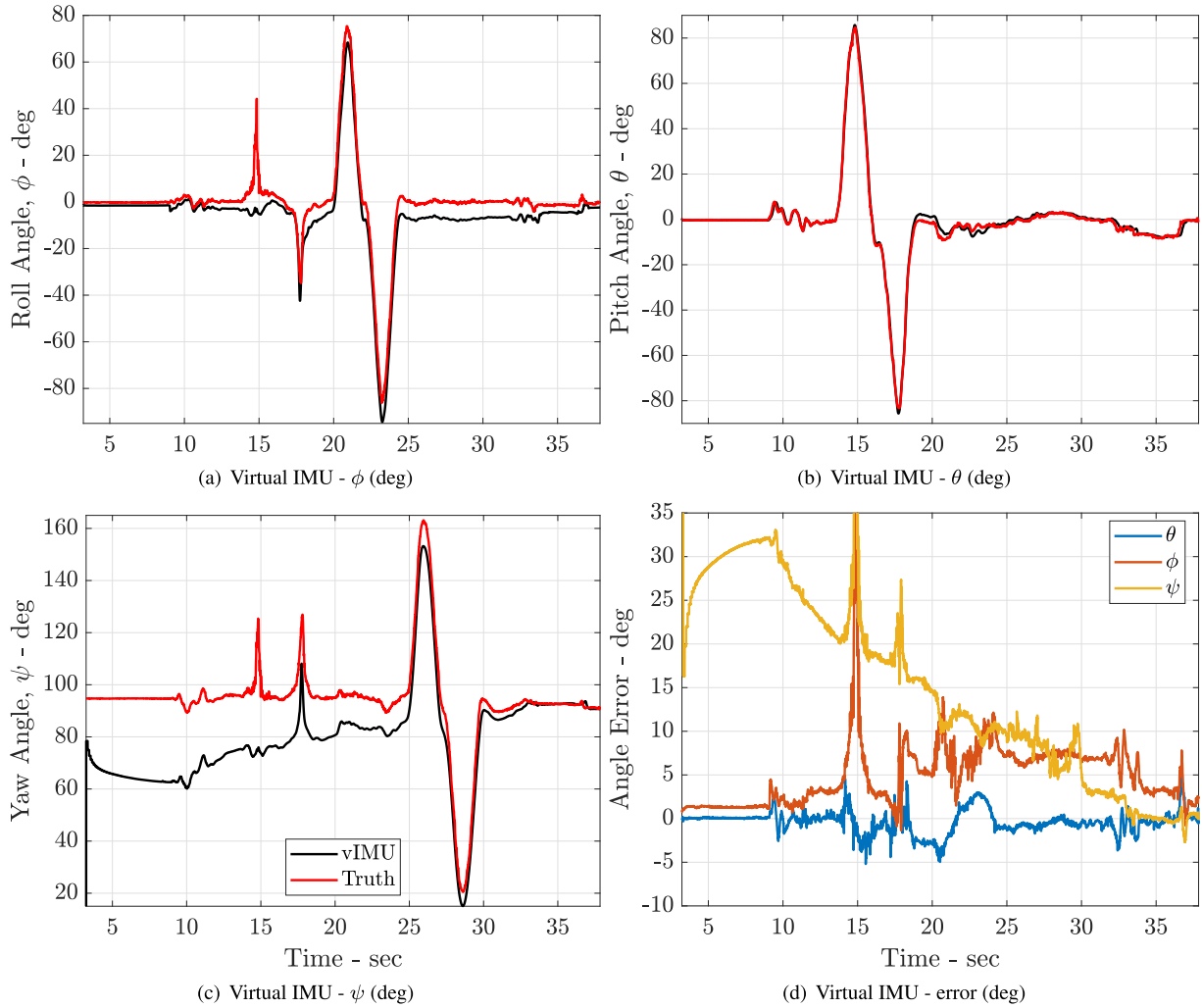
FIGURE 4. State comparison between virtual IMU filter and motion tracker.

obtained from onboard estimation and motion capture system were time synced by an impulse strike at the start of test.

All the state estimators were initialized at zero state quaternion, with alignment correction using magnetometer. Conservative measurement noise covariances were chosen for the simulation.

For more intuitive interpretation and clear visual comparison all the plots described below are plotted in Tait-Bryan angles (body 3-2-1 SO(3) rotation [35])

$$\begin{bmatrix} \phi \\ \theta \\ \psi \end{bmatrix} = \begin{bmatrix} \texttt{atan2}(2(q_2q_3 + q_1q_4), 1 - 2(q_3^2 + q_4^2)) \\ -\texttt{asin}(2(q_2q_4 - q_1q_3)) \\ \texttt{atan2}(2(q_3q_4 + q_1q_2), 1 - 2(q_2^2 + q_3^2)) \end{bmatrix}, \quad (23)$$

with ψ as the heading angle of the aircraft, θ as the pitch angle of the aircraft and ϕ as the roll/bank angle, and the definition of quaternion is consistent with Eqn (12).

VI. EXPERIMENTAL IMPLEMENTATION
To illustrate the working and performances comparison of the outlined estimator fusions in this paper, the estimation

TABLE 1. Motive OptiTracker system specification [39].

Positional accuracy	± 0.2 mm
Rotational accuracy	± 0.1 deg

routines are implemented on an onboard unmanned aerial system (UAS) autopilot and compared to both onboard estimates using contemporary autopilots and external reference data. The UAS implements the proposed estimators using an onboard autopilot built on a Raspberry PI 3B+ platform running Navio2 which includes two IMUs (MPU9250 [36] and LSM9DS1 [37]). A Pixhawk 2.1 which includes additional three IMUs (2 MPU9250 and LSM303D [38]) running the contemporary Ardupilot estimator as well as logging raw IMU data is also mounted on the UAS and identifying markers are added to use an external motion capture system (OptiTracker) shown in Fig: (3) as a reference to expected results due to high accuracies as given in Table (1).

The data collected from all five IMUs at a rate of 200Hz are used as input to all the estimation fusion algorithms.
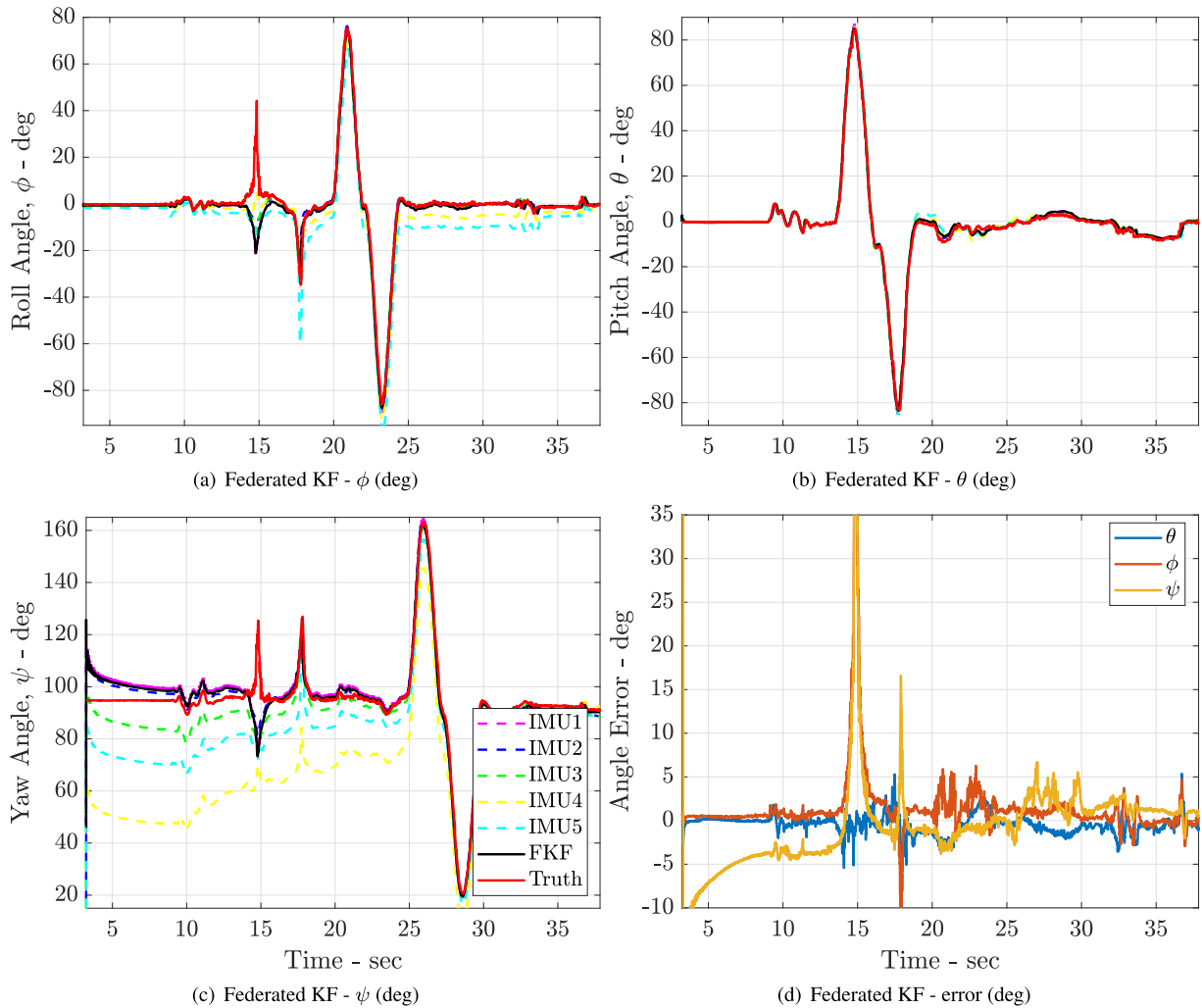
FIGURE 5. State comparison between Augmented Kalman Filter and motion tracker.

To evaluate the performance of the estimation routines all the state estimates are compared to the output from the motion capture system measurement at the same rate of 200Hz.

A. PERFORMANCE ANALYSIS IN MOTION CAPTURE ENVIRONMENT

To analyse the performance of each estimator fusion algorithms, described in this paper we find Root Mean Square Error (RMSE) for each formulation and compare it against the data obtained from motion capture system using

$$ RMSE = \sqrt{\sum_{i=0}^{i=N} \frac{(\hat{x}_i - x_i)^2}{N}}, \qquad (24) $$

with $\hat{x}_i$ being the estimates obtained from the state estimator formulations and x_i are the corresponding states obtained using motion capture system.

While motion capture was used as a reference, the formulation does not always represent the true attitude. In particular, the 43° pitch angle transient at 13sec does not reflect

true attitude and is related to underlying coordinate frame definition differences between the estimation routines and the motion capture (Optitracker) system's Robot Operating System (ROS) toolkit (right and left handed coordinate systems). The ROS toolkit is in widespread contemporary use and the un-altered data has been retained to provide a realistic comparison as can be observed in Fig. (4)-(7).

The random walk and the rate random walk for the gyroscope were found using 12 hour data collection and analysis using basic allan variance as described in Appendix B of $\sigma_{IMU1} = 0.006°/\sqrt{s}$, $\sigma_{IMU2} = 0.016°/\sqrt{s}$, $\sigma_{IMU3} = 0.0206°/\sqrt{s}$, $\sigma_{IMU4} = 0.012°/\sqrt{s}$, and $\sigma_{IMU5} = 0.0231°/\sqrt{s}$.

1) COMPARISON OF vIMU TO MOTION TRACKING

When running vIMU routine we combine all the measurements into one single measurement with expected noise reduction and hence, we only have one output for comparison. As there is only one local filter calculation taking place we expect computational load for this method to be minimum.
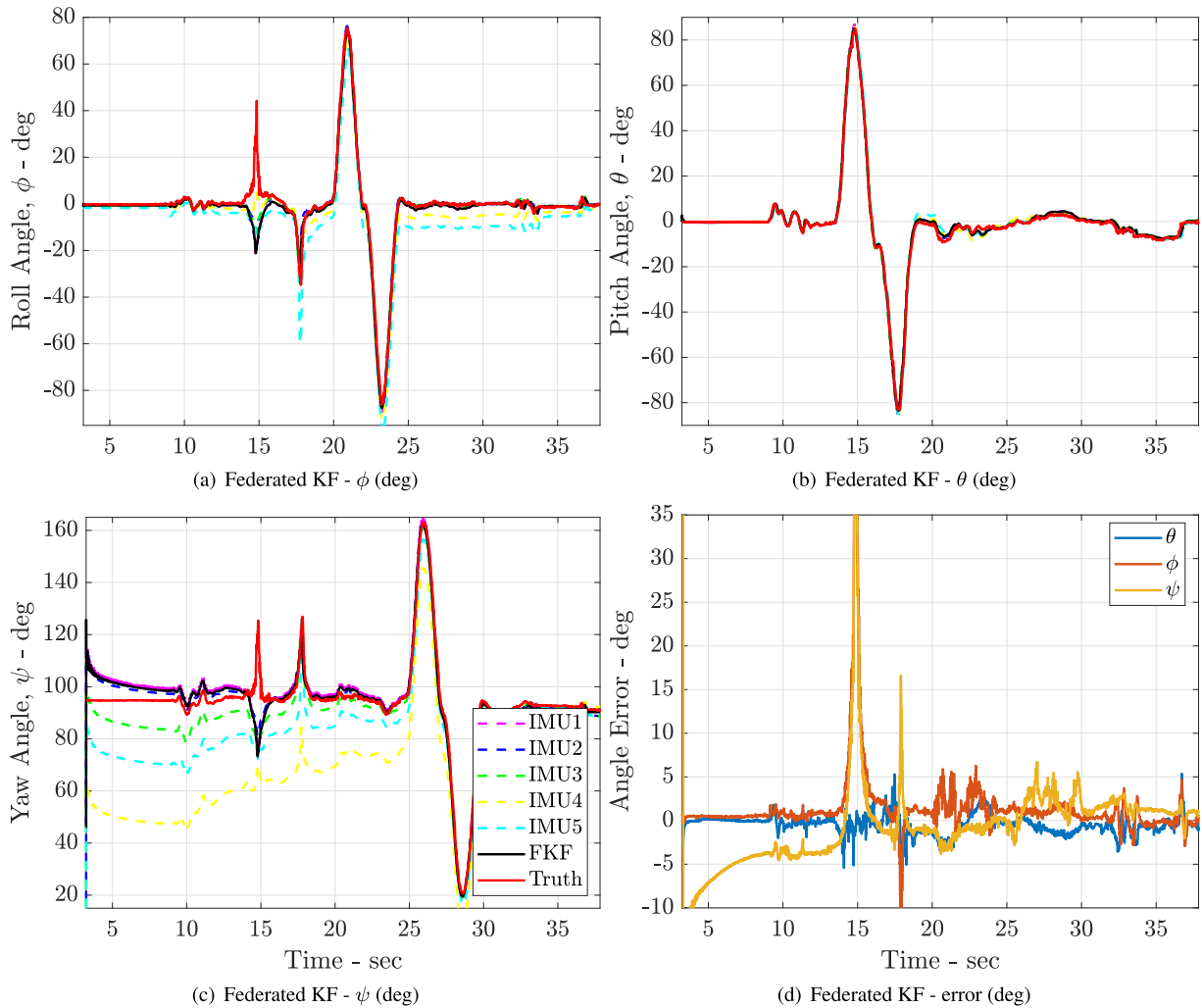
FIGURE 6. State comparison between Federated Kalman Filter, single IMU run, and motion tracker.

As shown in Fig. 4(a)- 4(c), the vIMU tracks θ very well compared to ϕ and ψ. The experiment was conducted indoors deviation from true ψ is expected. The RMSE values of all states using equation (24) are as shown in Fig. 4(d) and Table (2). We also see coupled effects between estimates. The deviation in ψ coupled with other estimates. This behaviour is expected as all the measurements were combined before the fusion and hence, there is only one input.

2) COMPARISON OF AKF TO MOTION TRACKING
AKF is very similar in implementation as vIMU, but instead of combining measurements before fusing it to state estimates, AKF uses all the measurements simultaneously in its measurement matrix and is computationally heavier than vIMU. Even though it is computationally heavy the state estimation is not as accurate as seen from Fig. 5(a)- 5(c)

AKF deviates from its estimates during rapid motions near the time synchronization impulses. AKF estimates deviates

significantly when ψ is far from the reference. The RMSE values of all states using equation (24) are as shown in Fig. 5(d) and Table (2).

3) COMPARISON OF FKF TO MOTION TRACKING
State estimates from the FKF are shown in Fig. 6(a)- 6(c). FKF best tracks the state estimates and even though experiment was conducted indoors FKF converges to the true ψ rapidly. The RMSE values of all states using equation (24) are as shown in Fig. 6(d) and Table (2). When compared to VIMU and AKF, FKF has lower estimate error. Moreover, as it uses the covariance matrix of each states to fuse the estimates there is no coupled deviations observed.

The FKF involves a larger number of computations than the other approaches as it requires individual state estimation and then is fused in one state estimation, but the advantage of FKF is that its structure allows easy integration of fault detection and individual sensor health monitoring.
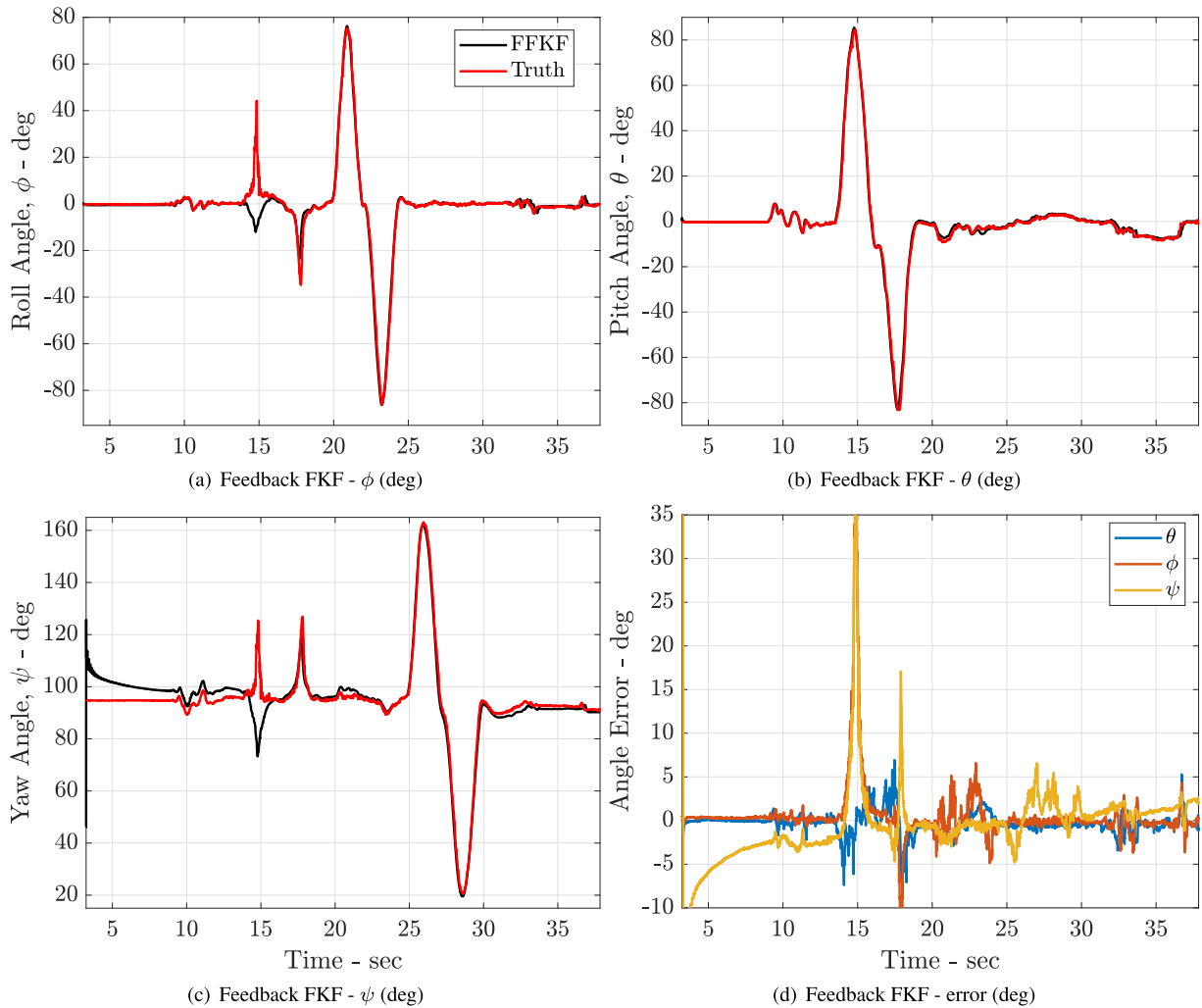
FIGURE 7. Comparison between feedback federated Kalman filter and motion tracker time histories.

4) COMPARISON OF FFKF TO MOTION TRACKING

The FFKF involves the same computational load as the FKF which is still larger than the other approaches as it requires individual state estimation and then is fused in one state estimation, FFKF holds all the advantages of FKF and still performs better than FKF.

State estimates from FKF are shown in Fig. 7(a)- 7(c). FFKF best tracks the state estimates and even though experiment was conducted indoors FFKF converges to the true ψ rapidly. The RMSE values of all states using equation (24) are as shown in Fig. 7(d) and Table (2). Since FFKF is an extension of FKF, same behaviour is observed but with better states estimates.

B. PERFORMANCE IN FLIGHT TEST

Now to see how all the state estimation perform in real flight condition the implemented frameworks were put on am radio controlled (E-Flite mpd Commander) aircraft. The performance of multi-IMU estimation cannot be directly measured quantitatively and hence, we use a qualitative comparison

against single-IMU estimation. The single-IMU estimation was performed on Pixhawk at 200Hz and data for 5 IMUs were recorded in the same configuration as mentioned above at 200Hz.

The flight was performed at ambient condition with wind speeds ranging from 8-10knots. This condition provided noise characteristics ideal for attitude estimator testing. The flight trajectory was freely chosen by a manual pilot and covered the full attitude envelope. An example of the attitude time history is shown in Fig. 8(a)- 8(b).

Fig. 8(a) shows that the bank angle estimate is generally consistent across all estimator frameworks, with deviations primarily at 537-540 seconds, likely due to normalization differences in magnetometer calibrations. Fig. 8(b) shows that the Pixhawk attitude estimates are an outlier, deviating at 5, 530, and 537 seconds. Although the Pixhawk estimate deviates from the multi-IMU estimates, the lack of an external attitude reference, combined with the deviations in all estimates at 520-525 and 532 seconds do not support
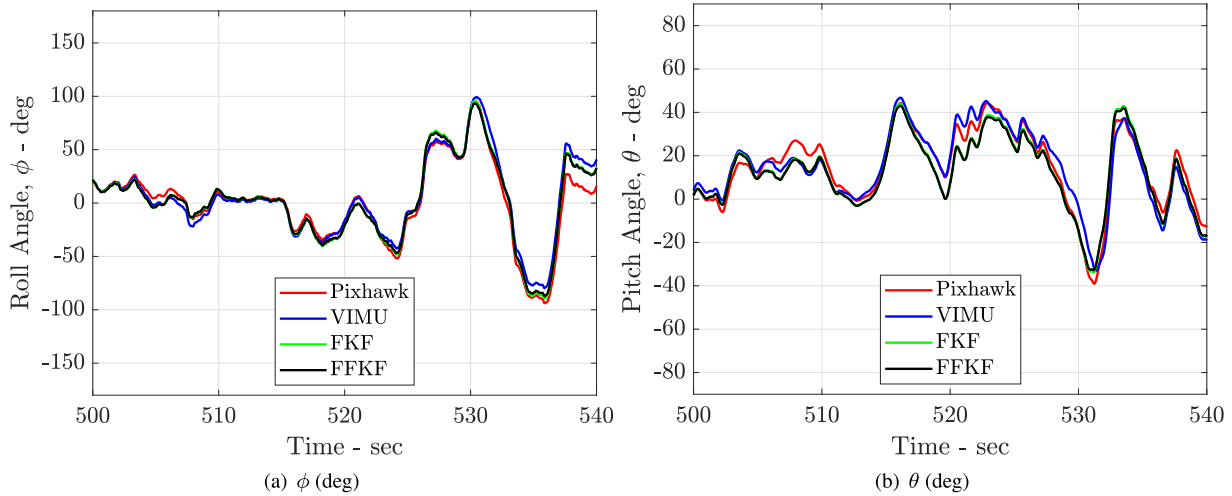
FIGURE 8. State comparison between Pixhawk state estimation, and multi-IMU state estimation.
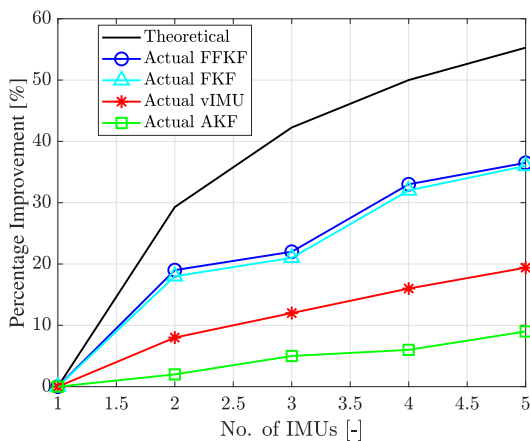

FIGURE 9. Idealized and experimentally implemented multi-IMU estimator performance for varying approaches.

TABLE 2. Measured state error.

Parameter	FFKF (deg)	FKF (deg)	vIMU (deg)	AKF (deg)
Error in ϕ	4.0229	4.793	6.180	15.748
Error in θ	1.168	1.190	1.371	7.100
Error in ψ	5.8813	5.878	19.102	19.892

FIGURE 10. Uncalibrated magnetometer.

FIGURE 11. Calibrated magnetometer.

a conclusion that multi-IMU estimator consistently outperforms the traditional single IMU case.

C. ESTABLISHED PERFORMANCE IMPROVEMENT

The actual experimental results demonstrated that feedback federated Kalman filter with attitude estimation using Bortz equation had the best performance as measured when compared to all the other methods. Table 2 shows the root mean square error for all the implemented runs using the 5 IMUs. Moreover, the estimators were tested independently using different IMUs as sensors to give the results shown in Fig. 9.
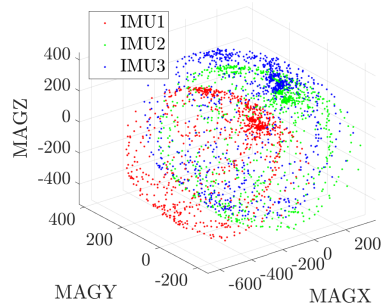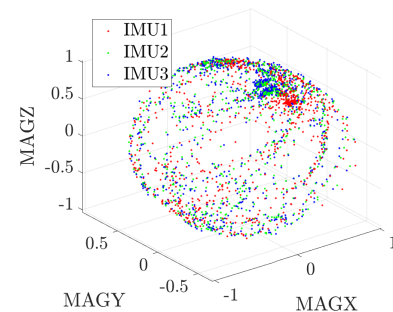
The results consistently indicate that Federated Kalman filter has the best improvement in state estimation accuracy no matter the number on IMU's employed.

VII. CONCLUSION

In this paper, the idea of fusing multiple IMU to improve the accuracy and reliability of the state estimation for UAS was investigated. Four state estimation fusion methods were tested with two different local attitude estimators. The state
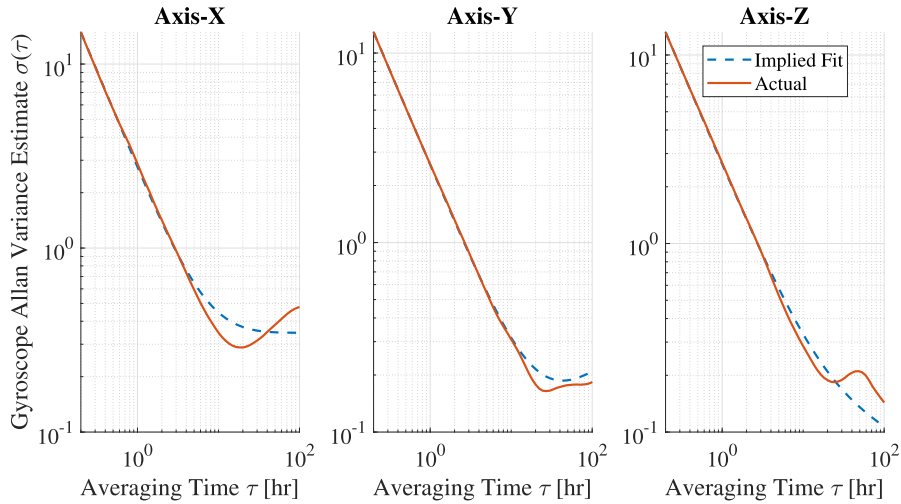
FIGURE 12. Single-axis-gyro PSD with frequency averaging.

estimators were then implemented on data collected from 5 different IMU's (2 from Navio2 on Raspberry Pi, and 3 from Pixhawk 2.1). The estimators were tested against the reference data obtained using motion tracker system (OptiTracker).

The results obtained in this paper clearly show the potential of employing multi-IMU based state estimation to not only improve the accuracy of the estimates and also to add redundancies in the system. Future work includes the extension of the studies attitude estimation to include on board wind speed estimation for UAS and having multiple decentralized agents to do wind field estimation.

APPENDIX A
MAGNETOMETER CALIBRATION
Magnetometer calibration for multi-IMU was based on the routine outlined by Ozyagcilar [40], which corrects for hard and soft iron interference. The calibration process consists of fitting a set of ten model parameters to the magnetometer measurements. Four parameters model the hard-iron offset, six model the soft-iron matrix and one models the geomagnetic field strength.

In the multi-IMU case, the magnetometers used in the experiment are not identical and can have biases and offsets. After the calibration parameters were identified, a normalization was implemented to adjust for individual magnetometer scale variations. Fig. 10 shows an example of the magnetometer reading during a rotation about all axes before calibration and Fig. 11 shows the same calibration loop corrected for both hard and soft interference.

APPENDIX B
ALLAN DEVIATION
The Allan deviation plot is a method of graphing the various error sources of a time-series of data on a single plot. The method was first introduced by David Allan in 1966 to

measure the frequency stability of clocks and oscillators. The technique is useful for inertial navigation systems since it allows both the angle/velocity random walk and bias stability of the sensors to be determined in a single plot.

To compute the Allan deviation for a time series of data x_i, begin by splitting the data series into bins of size n where N is the number of resulting bins. Let y_i be the average of bin i where $i = 1, \ldots, N$. The Allan variance of x_i is given by

$$\sigma^2(\tau) = \frac{1}{2(N-1)} \sum_{1}^{N-1} (x_{i+1} - xi)^2$$

where τ is the time constant for consecutive samples in x_i. The Allan deviation then is found by taking the square root of the Allan variance. For interpretation of the Allan deviation plot, please refer to [[30], [41]].

REFERENCES
[1] J. González-Rocha, C. A. Woolsey, C. Sultan, and S. F. J. De Wekker, "Sensing wind from quadrotor motion," *J. Guid., Control, Dyn.*, vol. 42, no. 4, pp. 836–852, Apr. 2019.
[2] J. C. McMillan, J. S. Bird, and D. A. G. Arden, "Techniques for soft-failure detection in a multisensor integrated system," *Navigation*, vol. 40, no. 3, pp. 227–248, Sep. 1993.
[3] Y. Beaudoin, A. Desbiens, E. Gagnon, and R. Landry, "Satellite launcher navigation with one versus three IMUs: Sensor positioning and data fusion model analysis," *Sensors*, vol. 18, no. 6, p. 1872, Jun. 2018.
[4] C. W. Kang and C. G. Park, "A soft-failure detection and identification algorithm for the integrated navigation system of lunar lander," *Proc. Inst. Mech. Eng., G, J. Aerosp. Eng.*, vol. 230, no. 11, pp. 2023–2035, Sep. 2016.
[5] I. Skog, J.-O. Nilsson, and P. Handel, "An open-source multi inertial measurement unit (MIMU) platform," in *Proc. Int. Symp. Inertial Sensors Syst. (ISISS)*, Feb. 2014, pp. 1–4.
[6] I. Skog, J.-O. Nilsson, and P. Händel, "Pedestrian tracking using an IMU array," in *Proc. IEEE Int. Conf. Electron., Comput. Commun. Technol. (CONECCT)*, Jan. 2014, pp. 1–4.
[7] M. Tanenhaus, T. Geis, D. Carhoun, and A. Holland, "Accurate real time inertial navigation device by application and processing of arrays of MEMS inertial sensors," in *Proc. IEEE/ION Position, Location Navigat. Symp.*, May 2010, pp. 20–26.
[8] J. Zhang and H. Ji, "Distributed multi-sensor particle filter for bearings-only tracking," *Int. J. Electron.*, vol. 99, no. 2, pp. 239–254, Feb. 2012.

[9] C. Gao, G. Zhao, J. Lu, and S. Pan, "Decentralised moving-horizon state estimation for a class of networked spatial-navigation systems with random parametric uncertainties and communication link failures," *IET Control Theory Appl.*, vol. 9, no. 18, pp. 2666–2677, Dec. 2015.

[10] K. Eckenhoff, P. Geneva, and G. Huang, "Sensor-failure-resilient multi-IMU visual-inertial navigation," in *Proc. Int. Conf. Robot. Automat. (ICRA)*, May 2019, pp. 3542–3548.

[11] A. Waegli, S. Guerrier, and J. Skaloud, "Redundant MEMS-IMU integrated with GPS for performance assessment in sports," in *Proc. IEEE/ION Position, Location Navigat. Symp.*, May 2008, pp. 1260–1268.

[12] I. Colomina, M. Giménez, J. Rosales, M. Wis, A. G. Mez, and P. Miguelsanz, "Redundant IMUs for precise trajectory determination," Inst. Geomatics, Barcelona, Spain, Tech. Rep. 16834739, 2004.

[13] R. H. Rogne, T. H. Bryne, T. I. Fossen, and T. A. Johansen, "Redundant MEMS-based inertial navigation using nonlinear observers," *J. Dyn. Syst., Meas., Control*, vol. 140, no. 7, Jul. 2018, Art. no. 071001.

[14] B. M. Scheninger, J. J. Hutton, and J. C. McMillan, "Low cost inertial/GPS integrated position and orientation system for marine applications," *IEEE Aerosp. Electron. Syst. Mag.*, vol. 12, no. 5, pp. 15–19, May 1997.

[15] J. B. Bancroft and G. Lachapelle, "Data fusion algorithms for multiple inertial measurement units," *Sensors*, vol. 11, no. 7, pp. 6771–6798, 2011.

[16] J. N. Gross, Y. Gu, M. B. Rhudy, S. Gururajan, and M. R. Napolitano, "Flight-test evaluation of sensor fusion algorithms for attitude estimation," *IEEE Trans. Aerosp. Electron. Syst.*, vol. 48, no. 3, pp. 2128–2139, Jul. 2012.

[17] S. Sukkarieh, P. Gibbens, B. Grocholsky, K. Willis, and F. H. Durrant-Whyte, "A low-cost, redundant inertial measurement unit for unmanned air vehicles," *Int. J. Robot. Res.*, vol. 19, no. 11, pp. 1089–1103, Nov. 2000.

[18] Y. N. Bezkorovainyi and O. A. Sushchenko, "Improvement of UAV positioning by information of inertial sensors," in *Proc. IEEE 5th Int. Conf. Methods Syst. Navigat. Motion Control (MSNMC)*, Oct. 2018, pp. 123–126.

[19] M. Givens, C. Coopmans, and R. Christensen, "An estimation-domain approach to MEMS multi-IMU fusion for sUAS," in *Proc. Int. Conf. Unmanned Aircr. Syst. (ICUAS)*, Jun. 2019, pp. 1048–1053.

[20] Y. Beaudoin, A. Desbiens, E. Gagnon, and R. Landry, "Satellite launcher navigation with one versus three IMUs: Sensor positioning and data fusion model analysis," *Sensors*, vol. 18, no. 6, p. 1872, Jun. 2018.

[21] P. S. Marinushkin and I. A. Podshivalov, "MEMS-based non-orthogonal redundant inertial measurement unit for miniature navigation systems," in *Proc. Int. Siberian Conf. Control Commun. (SIBCON)*, May 2015, pp. 1–3.

[22] J. B. Bancroft, "Multiple inertial measurement unit fusion for pedestrian navigation," Univ. Calgary, Calgary, AB, Canada, Tech. Rep., 2011, doi: 10.11575/PRISM/3915.

[23] N. A. Carlson, "Federated square root filter for decentralized parallel processors," *IEEE Trans. Aerosp. Electron. Syst.*, vol. 26, no. 3, pp. 517–525, May 1990.

[24] A. Brown and M. A. Sturza, "The effect of geometry on integrity monitoring performance," in *Proc. ION GPS*, 1990, pp. 121–129.

[25] M. E. Pittelkau, "Rotation vector in attitude estimation," *J. Guid., Control, Dyn.*, vol. 26, no. 6, pp. 855–860, Nov. 2003.

[26] M. A. Sturza, "Navigation system integrity monitoring using redundant measurements," *Navigation*, vol. 35, no. 4, pp. 483–501, 1988.

[27] C. I. Oliver, "Functions of random variables," in *Fundamentals of Applied Probability and Random Processes*, O. C. Ibe, Ed., 2nd ed. Boston, MA, USA: Academic, 2014, ch. 6, pp. 185–223.

[28] M. Lovric, Ed., *International Encyclopedia of Statistical Science*. Berlin, Germany: Springer, 2011.

[29] N. A. Carlson and M. P. Berarducci, "Federated Kalman filter simulation results," *Navigation*, vol. 41, no. 3, pp. 297–322, 1994.

[30] *IEEE Standard Specification Format Guide and Test Procedure for Coriolis Vibratory Gyros*, IEEE Standard 1431-2004, 2004, pp. 1–78.

[31] J. Bortz, "A new mathematical formulation for strapdown inertial navigation," *IEEE Trans. Aerosp. Electron. Syst.*, vol. AES-7, no. 1, pp. 61–66, Jan. 1971.

[32] A. Khosravian, J. Trumpf, R. Mahony, and T. Hamel, "Recursive attitude estimation in the presence of multi-rate and multi-delay vector measurements," in *Proc. Amer. Control Conf. (ACC)*, Jul. 2015, pp. 3199–3205.

[33] T. R. Kane and L. A. David, *Dynamics: Theory and Applications*. New York, NY, USA: McGraw-Hill, 2005.

[34] Y. Yang and W. Gao, "An optimal adaptive Kalman filter," *J. Geodesy*, vol. 80, no. 4, pp. 177–183, 2006.

[35] A. M. Zamorzaev and A. F. Palistrant, "Rotations, quaternions and double groups by S. Altmann," *Acta Crystallographica A, Found. Crystallogr.*, vol. 44, no. 4, p. 622, 1988.

[36] *MPU-9250 Product Specification, Revision 1.1*, TDK, Tokyo, Japan, 2016.

[37] *iNEMO Inertial Module: 3D Accelerometer, 3D Gyroscope, 3D Magnetometer, Revision 3*, STMicroelectronics, Geneva, Switzerland, 2015.

[38] *Ultra-Compact High-Performance eCompass Module: 3D Accelerometer and 3D Magnetometer Revision 2*, STMicroelectronics, Geneva, Switzerland, 2013.

[39] *NaturalPoint Product Documentation Version 2.3*, OptiTrack-Motion Capture Syst., USA, 2021.

[40] T. Ozyagcilar, "Calibrating an ecompass in the presence of hard and soft-iron interference," Freescale Semicond., Eindhoven, The Netherlands, Tech. Rep. AN4246, 2015.

[41] *IEEE Standard Specification Format Guide and Test Procedure for Linear, Single-Axis, Pendulous, Analog Torque Balance Accelerometer*, IEEE Standard 337-1972, 1972, pp. 1–48.
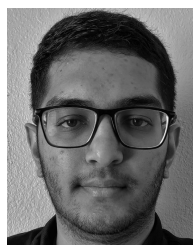
UJJVAL N. PATEL received the B.S. degree in mechanical engineering and aerospace engineering from Oklahoma State University, Stillwater, OK, USA, in 2019, where he is currently pursuing the M.S. degree in mechanical and aerospace engineering.

His research interests include control theory, estimation theory, and multiagent systems.

IMRAAN A. FARUQUE received the B.S. and C.S. degrees in aerospace and ocean engineering from Virginia Polytechnic Institute and State University, Blacksburg, VA, USA, in 2006, and the M.S. and Ph.D. degrees in aerospace engineering from the University of Maryland, College Park, MD, USA, in 2010 and 2011, respectively.

He was a Founding Member of two university UAS test sites. He is currently an Assistant Professor with the School of Mechanical and Aerospace Engineering, Oklahoma State University, Stillwater, OK, USA. He is the Area Lead for autonomy with the OSU Unmanned Systems Research Institute, Stillwater. His research group is studying the flexible decision-making in insects during multiagent group and swarm flight, including developing experimentally consistent, mathematically rigorous, and models of insect feedback in groups and translating those strategies to engineered flight on unmanned aerial vehicles. His research interests include reduced-order models of complex systems, biologically inspired locomotion and control systems, unmanned aerial systems, and flight dynamics and control.

Prof. Faruque is a member of the OSU Brain Initiative and the Oklahoma Aerospace Institute for Research and Education (O AIRE). He was a recipient of the 2019 ONR Young Investigator Award and the 2017 American Institute of Aeronautics and Astronautics NCS Young Engineer/Scientist of the Year Award.

• • •